

Numerical Analysis of Wave Load Characteristics on Jack-Up Production Platform Structure Using Modified $k-\omega$ SST Turbulence Model

Gilang Muhammad¹, Nu Rhahida Arini², Eko Charnius Ilman³,
Teguh Hady Ariwibowo²

¹Electrical Engineering, Politeknik Elektronika Negeri Surabaya, Surabaya, Indonesia

²Power Plant Engineering Study Program, Politeknik Elektronika Negeri Surabaya,
Surabaya, Indonesia

³Ocean Engineering, Bandung Institute of Technology, Bandung, Indonesia
Corresponding Author: arini@pens.ac.id

Received January 10, 2023; Revised March 20, 2023; Accepted June 9, 2023

Abstract

One of the important stages in the offshore structure design process is the evaluation of the marine hydrodynamic load in which the structure operates, this is to ensure an appropriate design and improve the safety of the structure. Therefore, accurate modeling of the marine environment is needed to produce good evaluation data, one of the methods that can accurately model the marine environment is through the Computational Fluid Dynamic (CFD) method. This research aims to analyze the ocean wave load of pressure and force characteristics on the jack-up production platform hull structure using the (CFD) method. The foam-extend 4.0 (the fork of the OpenFOAM) software with waveFoam solver is utilized to predict the free surface flow phenomena as its capability to predict with accurate results. The Reynold Averaged Navier Stokes (RANS) turbulence model of $k-\omega$ SST is applied to predict the turbulence effect in the flow field. Five variations of incident wave direction type are carried out to examine its effect on the pressure and force characteristics on the jack-up production platform hull. The wave model shows inaccurate results with the decrease in wave height caused by excessive turbulence in the water surface area. Excessive turbulence levels can be overcome by incorporating density variable and buoyancy terms based on the Standard Gradient Diffusion Hypothesis (SGDH) into the turbulent kinetic energy equation. The $k-\omega$ SST Buoyancy turbulence model shows accurate results when verified to predict wave run-up and horizontal force loads on monopile structures. Furthermore, test results of the wave load on the jack-up production platform hull structure shows that the most significant wave load is obtained in variations with the wave arrival direction relatively opposite to the platform wall. Especially in the direction of 90° because it also has the most expansive impact surface area. Meanwhile, the lower wave load is obtained in variations 45° and 135° , which have the relatively oblique direction of wave arrival to the surface.

Keywords: Jack-Up Production Platform, $k-\omega$ SST, CFD, OpenFOAM, Wave.

1. INTRODUCTION

Petroleum and natural gas are fossil fuels that are essential sources of energy because oil and gas have a significant proportion in meeting the world's energy consumption. The process to obtain the oil and an exploitation process carries out natural gas through proven oil or gas wells [1].

One of the critical infrastructures in supporting the exploitation of oil and natural gas is production platform which is a utility to exploitate into underground reservoirs to obtain oil and natural [2]. This production platform can be located in various places according to the location of the oil or gas reservoir. The location of the oil well can be either onshore or offshore. Especially in offshore locations, supporting infrastructure is needed to support and operate drilling/production.

A jack-up production platform is one type of platforms that is widely used to support offshore oil and gas exploration activities due to its mobility advantages [3]. Because jack-up production platform can operate in extreme and unpredictable environment, the strength of the offshore production platform structure must be designed to withstand extreme conditions, especially against marine hydrodynamic loads such as wave loads and ocean currents, so it is necessary to assess the feasibility of the structural design before the platform is built [4–6].

The feasibility study of complex structural design related to fluid flow (fluid and structure interaction) can generally be carried out using two methods, namely the experimental method and the numerical method. The experimental research methods have the advantage of a good level of accuracy, but this must be supported by adequate test equipment and instruments so that they often require high costs along with the level of complexity of the case to be studied. The Deficiencies in the experimental method can be overcome by using numerical methods or Computational Fluid Dynamics (CFD). In the CFD method, besides having advantages in cost efficiency the validated numerical method produces prediction results that are quite accurate with higher detail of the property value to be observed [7,8].

Based on these problems, in the following research, a CFD modelling study will be carried out on an offshore jack-up production platform type with hydrodynamic loads on the hull waves to predict pressure loads and acting forces. CFD modelling will be carried out using OpenFOAM software, OpenFOAM is an open source CFD tool that has been used extensively in the field of fluid mechanics to predict phenomena that occur in fluid flow with accurate results. Research can be carried out more cheaply and effectively using the CFD method. Besides that, the CFD method advantage is that it can predict phenomena in fluid flow in more detail.

The Navier-Stokes equation is solved by the Reynold Averaged Navier Stokes (RANS) approach. The turbulent model of the two $k-\omega$ SST equations is applied in the following research because it has accurate results in

simulating fluid flow with a wide scope and has low computational costs. However, using a turbulent model in the free surface case with wave modelling produces an excessive turbulent effect on the surface area which can affect the shape of the wave profile created and decreases the accuracy of the simulation data. So that in the following research, modifications will also be made to the $k-\omega$ SST turbulence model to produce a free surface fluid flow simulation that can model waves and turbulence levels more accurately.

2. RELATED WORKS

There are many previous studies on fluid and structure interaction carried out using the CFD method with a good result such as work which was done by Arini [9], who has conducted research on the fluid-structure interaction of vertical axis tidal turbine blade. Several other studies examine the hydrodynamic loads of ocean waves on offshore structures using the CFD method, such as research conducted by Nizamani [10], who researched wave loads on decks by observing the vertical force parameters experienced by the decks. Meanwhile, Aggarwal [11] and Zeng [12] conducted a case simulation of breaking wave loads on monopile structures in waters with a slope; the parameters observed were horizontal forces on the structure. The validation process from the three studies by Nizamani, Aggarwal, and Zeng showed accurate results between the CFD simulation and experimental results; this shows the good reliability of the CFD method in modelling wave cases on free surface flow.

In free surface research with wave formation, the problem that often arises is weakening of the waves while simulating high steepness wave, this is caused by the excessive formation of turbulent kinetic energy in the near surface area when applying turbulence models, where the turbulence models is important when using the Reynold-Averaged Navier-Stokes (RANS) approach to produce accurate flow phenomena [13,14]. Devolder [15], tried to find a solution to this problem by modifying the turbulent model $k-\omega$ SST by including the density and buoyancy terms using Standart Gradient Diffusion Hypothesis (SGDH) into the turbulent equation with the aim of reducing the excessive level of turbulence in the water surface area. The wave CFD simulation of wave run up on monopile structure was carried out using the OpenFOAM CFD tool with the IHFOAM wave generator and absorber toolbox. The simulation results show relatively good accuracy with experiments and numerical results. Larsen & Fuhrman [16], also modified the $k-\omega$ turbulence model by adding limiter to stabilize and prevent the exponential formation of turbulent kinetic energy and kinematic viscosity. The results of the experiments show that wave formation results are relatively stable with longer simulation time and effectively prevent the exponential growth of turbulent kinetic energy and turbulent kinematic viscosity. Qu [17], conducted a comparative study of the turbulence model in the case of breaking waves in a monopile structure. Comparisons were made involving the modified $k-\omega$ based turbulence model by Devolder [15] and

Larsen & Fuhrman [16]. The results of the simulation show that modification of the $k-\omega$ SST turbulence model can produce turbulent kinetic energy results that are reasonable and accurate. Based on previous studies, the accuracy of the flow modelling in the case of free surface flow waves can be improved by modifying the parameters of the turbulent model used.

3. ORIGINALITY

The CFD modelling of offshore jack-up production platforms under ocean hydrodynamic wave loading was performed using OpenFOAM open-source software foam-extend 4.0 [18] with waveFoam solver to generate and absorb waves [19]. This research focused on the hull structure of the jack-up production platform to investigate pressure loads and forces on the hull when exposed to wave due to land subsidence and storms [20–22]. Five test cases were performed with different directions of ocean waves (0° , 45° , 90° , 135° , and 180°) to investigate the characteristic of pressure and force that act on the jack-up production platform hull with different wave impact direction. Furthermore, the modification of the $k-\omega$ SST turbulent model based on the more advanced buoyancy term, the Standard Gradient Diffusion Hypothesis (SGDH), is applied to overcome the decrease in incoming wave height due to excessive turbulence [15]. Before being applied to the case of the jack-up platform, the use of modification of the $k-\omega$ SST turbulent model was verified with the experimental case of wave on the monopile structure which is conducted by De Vos [23].

4. SYSTEM DESIGN

4.1 Numerical Method

4.1.1 Governing Equation

Navier Stokes equations are the fundamental equation for fluid flow that consist of average mass conservation equation and average momentum equation. The average mass conservation in Equation (1) and average momentum in Equation (2) for incompressible flow can be written as follows [24]:

$$\nabla \cdot \bar{\mathbf{u}} = 0 \quad (1)$$

$$\frac{\partial \bar{\mathbf{u}}}{\partial t} + \nabla \cdot (\bar{\mathbf{u}}\bar{\mathbf{u}}) - \nabla \cdot (\nu \nabla \bar{\mathbf{u}}) = -\bar{P} - \nabla \cdot (\bar{\mathbf{u}}'\bar{\mathbf{u}}') \quad (2)$$

4.1.2 Volume of Fluid (VOF)

The interface between the water surface and the air is obtained from the Volume of Fluid (VoF) method. The VoF method is based on the volume fraction where is 0 for air-filled cells, 1 for water-filled cells, and between 0 and 1 for water-air interface cells [25]. The volume fraction is solved using the advection Equation (3) below:

$$\frac{\partial \alpha}{\partial t} + \nabla \cdot (u\alpha) + \nabla \cdot (u_r \alpha (1 - \alpha)) = 0 \quad (3)$$

Where the (u_r) is artificial compressive velocity field.

4.1.3 Turbulence Model of k- ω SST

The turbulent model that is widely used in cases of high Reynold numbers and multiphase flow is the k- ω SST turbulence model, which consists of two transport equations for turbulent dissipation rate (ω) in Equation (4) and turbulent kinetic energy (k) in Equation (5) as follows [26]:

$$\begin{aligned} \frac{\partial \omega}{\partial t} + \nabla \cdot (\bar{u}\omega) - \omega \nabla \cdot \bar{u} - \nabla \cdot ((\alpha_\omega v_t + \mu) \nabla \omega) \\ = \gamma \min \left[S_2, \frac{c_1}{a_1} \beta^* \omega \max(a_1 \omega, b_1 F_{23} \sqrt{S_2}) \right] - \beta \omega^2 \\ + (1 - F_1) CD_{k\omega} \end{aligned} \quad (4)$$

$$\frac{\partial k}{\partial t} + \nabla \cdot (\bar{u}k) - k \nabla \cdot \bar{u} - \nabla \cdot ((\alpha_k v_t + \mu) \nabla k) = \min(G, c_1 \beta^* k \omega) - \beta^* k \omega \quad (5)$$

$$\mu_t = \frac{a_1 k}{\max \left[a_1 \omega, b_1 F_{23} \sqrt{2} \left[\frac{1}{2} (\nabla \bar{u} + (\nabla \bar{u})^T) \right] \right]} \quad (6)$$

Where $a_1 = 0.31$, $b_1 = 1$, $c_1 = 10$, and $\beta^* = 0.09$ are the closure coefficients. Turbulent viscosity for the k- ω SST equation is found using Equation (6). For the other coefficients are described in the following equation:

$$G = \mu_t S_2 \quad (7)$$

$$S_2 = 2 \left| \frac{1}{2} (\nabla \bar{u} + (\nabla \bar{u})^T) \right|^2 \quad (8)$$

$$CD_{k\omega} = 2\alpha_{\omega 2} \frac{\nabla k \cdot \nabla \omega}{\omega} \quad (9)$$

The k- ω SST combines the two properties of the k- ω and k- ϵ turbulent models, in which the turbulent model can have the same properties as k- ω for locations near walls and have k- ϵ properties for free flow [26]. The changing properties of the k- ω SST turbulent model are determined by the blending function, which in the k- ω SST equation is used for γ , β , α_k , and α_ω . The blending function equation is described in Equation (10) below:

$$\phi = F_1 \phi_1 + (1 - F_1) \phi_2 \quad (10)$$

For the coefficient values of ϕ_1 and ϕ_2 are provided in Table 1:

Table 1. Blending function coefficients

ϕ	α_k	α_ω	γ
ϕ_1	0.85	0.5	0.55
ϕ_2	1	0.856	0.44

4.1.4 Buoyancy Turbulence Model of k- ω SST

In the following research, the modification of the k- ω SST equation was carried out. The first modification was carried out by entering the density variable into the k and ω transport equations. This is because the original k- ω SST equation do not accommodate multiphase flow with various densities. Then the second modification was carried out by adding the buoyancy term (G_b) variable based on the Standard Gradient Diffusion Hypothesis (SGDH) implicitly into the k (G_{bk}) transport equations based on research by Devolder [15], who made modifications to the k- ω SST turbulent model in the case of wave run-up over monopile. The idea behind this modification is to force the turbulent kinetic energy and its formation frequency to be small in areas with a density gradient, resulting in a small turbulent kinetic viscosity value and reducing the excessive turbulence level. The modified k- ω SST turbulence model for turbulent dissipation rate (ω) in Equation (11) and turbulent kinetic energy (k) in Equation (12) as follows:

$$\begin{aligned} \frac{\partial \rho \omega}{\partial t} + \nabla \cdot (\rho \bar{u} \omega) - \omega \nabla \cdot \rho \bar{u} - \nabla \cdot (\rho (\alpha_\omega v_t + v) \nabla \omega) \\ = \rho \gamma \min \left[S_2, \frac{c_1}{a_1} \beta^* \omega \max(a_1 \omega, b_1 F_{23} \sqrt{S_2}) \right] - \rho \beta \omega^2 \\ + \rho (1 - F_1) CD_{k\omega} \end{aligned} \quad (11)$$

$$\begin{aligned} \frac{\partial \rho k}{\partial t} + \nabla \cdot (\rho \bar{u} k) - k \nabla \cdot \rho \bar{u} - \nabla \cdot (\rho (\alpha_k v_t + v) \nabla k) = \min(\rho G, c_1 \beta^* \rho k \omega) \\ + G_{bk} - \rho \beta^* k \omega \end{aligned} \quad (12)$$

$$G_{bk} = -\frac{v_t}{\sigma_t} (\nabla \rho) g \quad (13)$$

Where the variable of σ_t is the modified buoyancy coefficient with the default value of 0.85.

4.2 Numerical Setup

4.2.1 Verification Case of Wave Run-Up on Monopile

The verification geometry in the following study is based on the experimental study of wave run-up on monopile structures conducted by De Vos [23]. The test was carried out on a laboratory scale with the domain length of 20 m, width of 0.75 m, and height of 0.8 m, for the water depth is 0.5 m, for the mesh topology configuration using the hexahedron dominant configuration with a total of 2.4 million cells. The computational domain and mesh topology can be seen in Figure 1 and Figure 2.

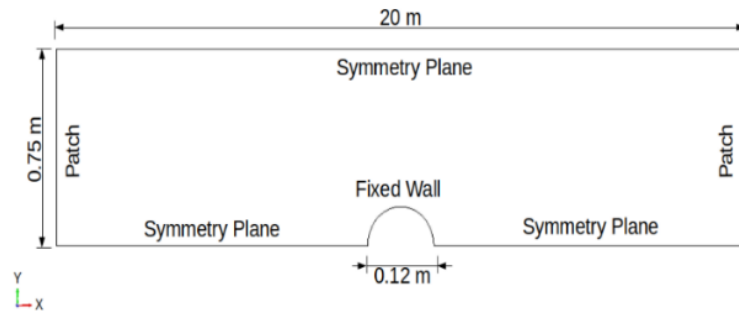


Figure 1. Computation domain and boundary condition of verification case

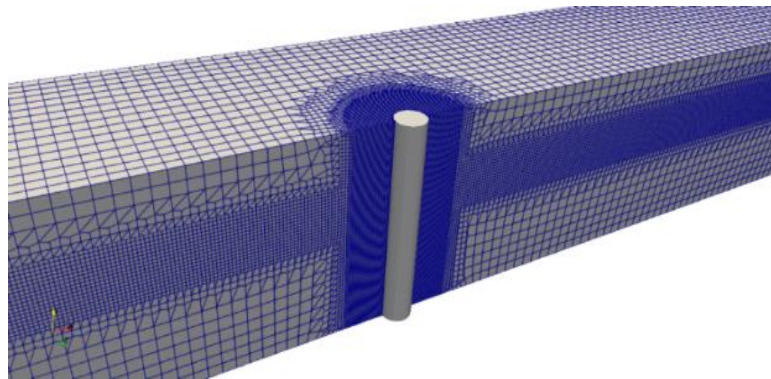


Figure 2. Verification domain mesh

4.2.2 Wave Load on Jack-up Production Platform Hull

The jack-up production platform geometry domain used in this study is simplified in the hull section, and it is assumed that there are no supporting legs and buildings, the geometry of jack-up production platform hull having the domain length of 53.6 m, 40.23 m width, and 6.1 m height, the location of the jack-up production platform hull is set to 50% of the wave amplitude above still water level. The geometry of the hull jack-up production platform, its position to the wave direction and water surface area can be seen in Figure 3-5.

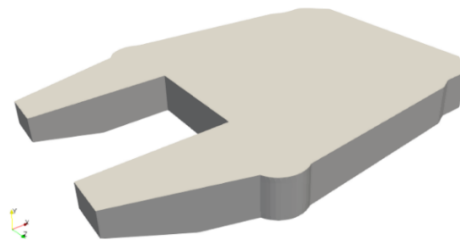


Figure 3. Isometric view of jack-up production platform hull geometry

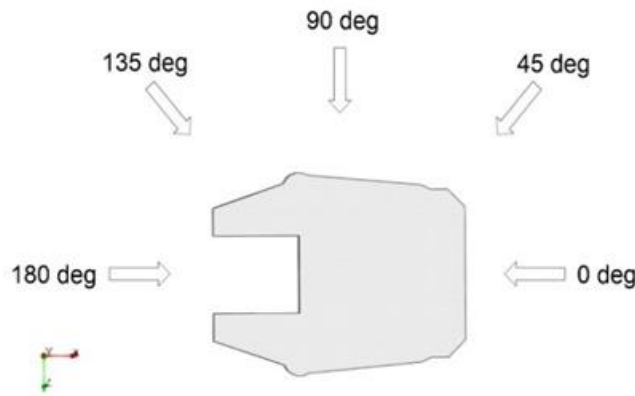


Figure 4. jack-up production platform hull position to the wave direction



Figure 5. jack-up production platform hull position to the wave and still water level

The total size of the computational domain has a length of 295 m, 100 m width, and 100 m height, with the water-filled domain of 70 m height and the remainder filled with air. In the inlet and outlet areas, there is the wave formation zone and wave absorption zone, the feature of the wave2Foam solver to generate and absorb waves. The formed mesh configuration uses hexahedron dominant topology containing 3.2 million cells. It has areas with the more significant number of cells with smaller cell sizes, especially near walls of the jack-up production platform hull and the water surface to capture the flow phenomenon more clearly. In addition to using the turbulent model, $k-\omega$ SST requires the $Y^+ \leq 1$ to get maximum results so that the cell size in the wall area will have high density. The boundary conditions, domain geometry, and mesh topology can be seen in Figure 6-8.

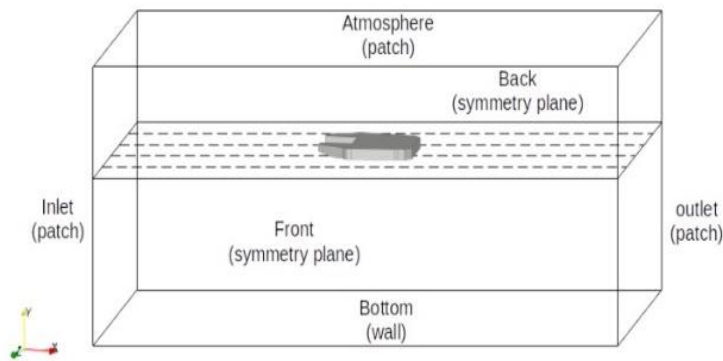


Figure 6. Jack-up production platform domain boundary condition

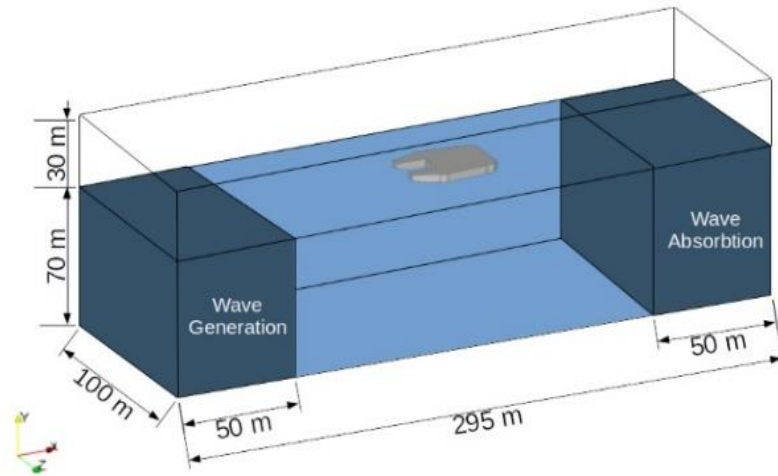


Figure 7. Full domain size

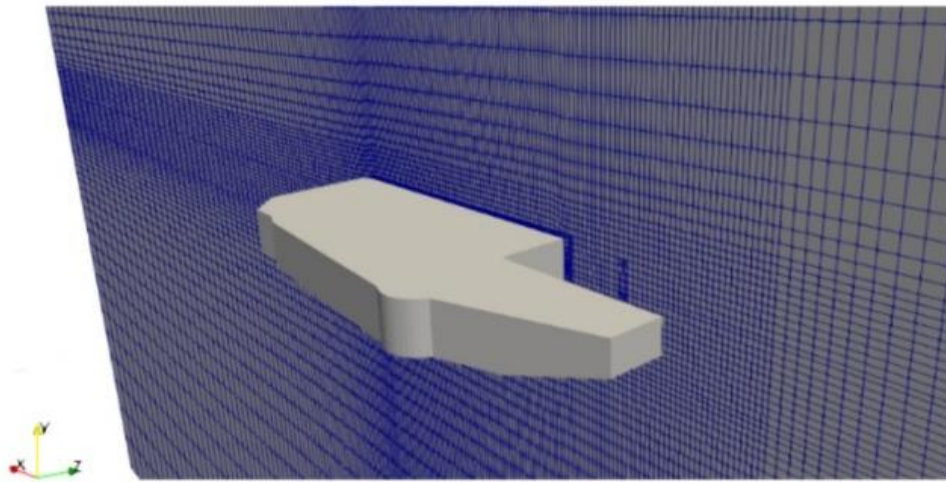


Figure 8. Jack-up production platform domain mesh

4.2.3 Fluid Properties and Numerical Scheme

Two-phase flow modelling with a wave model is simulated using OpenFOAM (foam-extend version 4.0) with the waveFoam solver. Before starting the iteration process, it is necessary to determine several parameters such as fluid properties and the Finite Volume scheme shown in Table 2-3.

Table 2. Fluid and wave properties

Parameter	Verification Case of Wave Run-Up on Monopile	Wave Load on Jack-Up Production Platform Hull
Fluid properties	<ul style="list-style-type: none"> Air $\rho = 1 \text{ kg/m}^3$ $\mu = 1.48 \times 10^{-5} \text{ kg/ms}$	<ul style="list-style-type: none"> Air $\rho = 1 \text{ kg/m}^3$ $\mu = 1.48 \times 10^{-5} \text{ kg/ms}$
	<ul style="list-style-type: none"> Water $\rho = 1000 \text{ kg/m}^3$ $\mu = 1 \times 10^{-6} \text{ kg/ms}$	<ul style="list-style-type: none"> Water $\rho = 1000 \text{ kg/m}^3$ $\mu = 1 \times 10^{-6} \text{ kg/ms}$
Viscous model	<ul style="list-style-type: none"> k-ω SST Buoyancy Modified k-ω SST Stable 	k- ω SST Buoyancy
Wave model	Stokes V	Stokes V
Wave specification	H = 0.12 m T = 1.05 s	H = 4 m T = 5.1 s

Table 3. Numerical scheme

Parameter	Verification Case of Wave Run-Up on Monopile	Wave Load on Jack-Up Production Platform Hull
Total time	35 s	80 s
Timestep	0.001 <i>max Delta T = 0.1</i>	0.001 <i>max Delta T = 0.1</i>
Courant number limit	0.25	0.25
Time discretization	Euler	Euler
Gradient scheme	linear	linear
Divergence scheme	upwind	upwind

The numerical setup in the verification and jack-up production platform case is similar to maintain the appropriate results. The difference between the verification and the jack-up production platform case is only in the total simulation duration due to the different domain sizes and wave specification. The wave specification in the verification case has the wave height of $H = 0.12 \text{ m}$ and the period of $T = 1.05 \text{ s}$, while in the case of the jack-up platform, it has the wave specification with the height of $H = 4 \text{ m}$ and the period of $T = 5.1 \text{ m}$. Although they have different specifications, the waves in the verification case and the jack-up production platform are of the same type, high-steepness waves and deep-sea waves. Furthermore, for the wave model selection using the Stokes V regular wave model based on the provisions of API RP 2A-WSD [27]. The value of the courant number is set at the maximum value of 0.25 to get accurate results. The simulation time step will adjust to the limit value of the courant number.

5. EXPERIMENT AND ANALYSIS

5.1 Wave Model Verification

Wave model verification is carried out to ensure the suitability of the model formed with the theoretical wave model. In the following research, the wave model verification process uses the jack-up production platform computational domain without involving the jack-up production platform geometry. In the wave model verification process, a comparison of the original $k-\omega$ SST and modified $k-\omega$ SST ($k-\omega$ SST Buoyancy) turbulence models was also conducted to test each turbulent model ability to model Stokes V waves according to specifications.

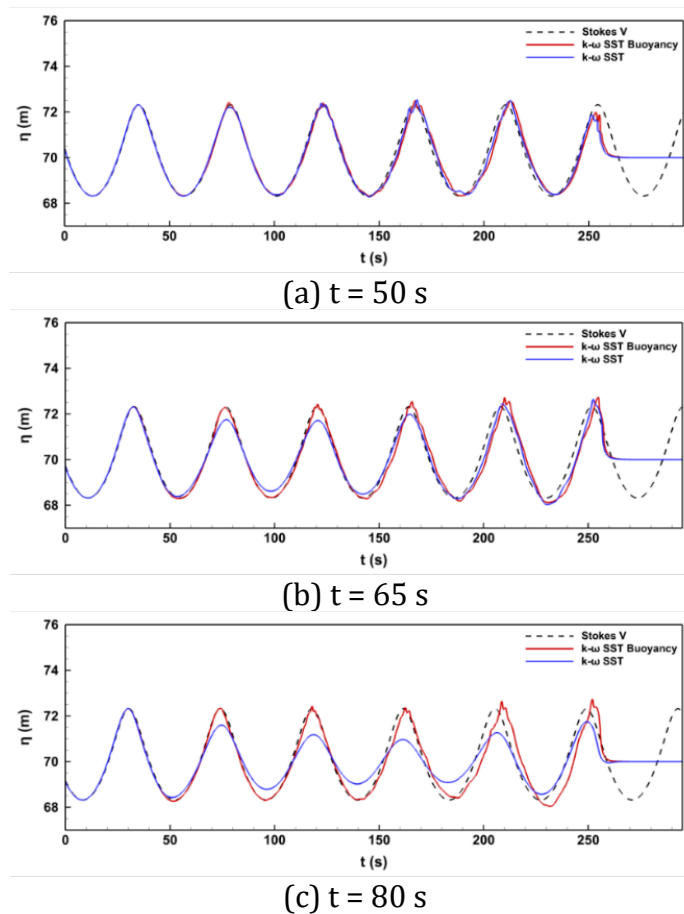


Figure 9. Comparison of the Stokes V wave profile at different times

Figure 9 shows the wave profile taken at the water surface with a depth of 70 m. The x-axis shows the position in the computational domain. At the end near the outlet area, there is a relaxation zone that functions to absorb waves so that the waves lose elevation. Based on the verification results of the Stokes V wave model that has been obtained, it is known that in the standard SST $k-\omega$ SST model, the elevation value decreases with increasing simulation time in Figure 9c. In contrast, the $k-\omega$ SST Buoyancy turbulent

model results can maintain the Stokes V wave profile for a longer simulation time.

The comparison plot of turbulent kinematic viscosity results in Figure 10. it shows the formation of a high turbulent kinematic viscosity accompanied by a decrease in wave height when using the original k- ω SST turbulent model. The increase in turbulent kinetic viscosity is due to friction from the air with water which triggers increasing turbulence energy in surface area with variations in density.

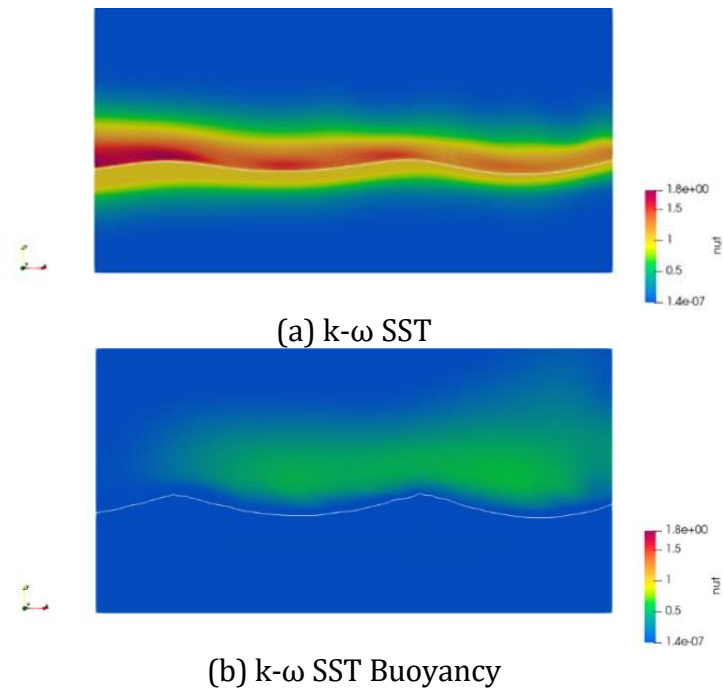


Figure 10. Turbulent kinematic viscosity ratio $\mu_t \left(\frac{m^2}{s^2} \right)$ at time $t = 80$ s and at positions $x = 147.5$ m to $x = 245$ m.

Furthermore, Figure 10b shows the results of the turbulent kinematic viscosity contour plot obtained with the k- ω SST Buoyancy turbulence model. It can be seen that the formation of turbulent kinematic viscosity is lower than when using the original k- ω SST turbulence model. The lower kinematic viscosity formation occurs due to the lower formation turbulent kinetic energy in the water surface area or areas with density gradient. The lower turbulent kinematic viscosity leads to the lower turbulence level so the wave can maintain its elevation, which is essential to ensure proper wave test load.

5.2 Wave Model Verification

The following verification stage compares the CFD simulation results with experimental case studies of fluid interactions with identical structures. This stage was carried out to test the ability of the modified k- ω SST Buoyancy turbulence model on fluid interaction with structures. The results of the CFD simulation will be compared with the results of experimental

testing from De Vos [23], who examined wave interaction on monopile structures. The compared data includes wave run-up data and the horizontal force. The wave run-up data collection is illustrated in Figure 11, where the data collection is divided into 3 positions around the surface of the cylinder.

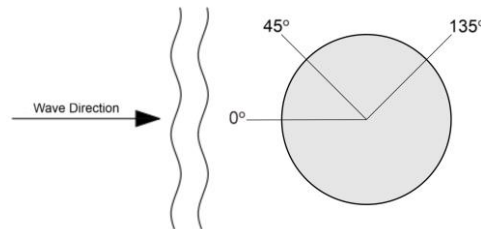


Figure 11. Data collection location of wave run-up from the top view of the cylinder

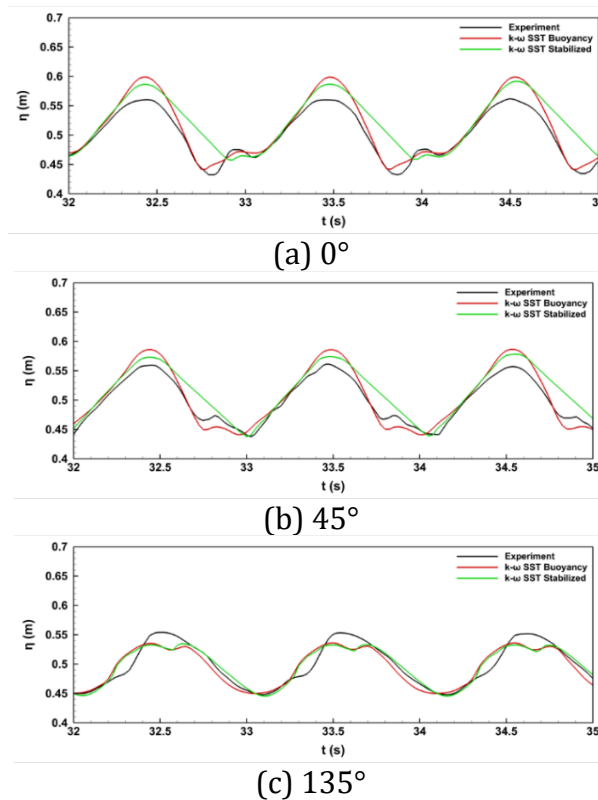


Figure 12. Wave run-up data from various positions

In the case of verifying the wave load on a vertical cylinder, a comparison of the results of the wave run-up modeling was carried out using the $k-\omega$ SST Buoyancy turbulence model and the modified $k-\omega$ SST Stable carried out by Qu [17]. The plot of the wave run-up data retrieval results is shown in Figure 12, where the duration of data retrieval is 3 seconds from 32 seconds to 35 seconds. Based on the wave run-up data obtained in Figure 8, it can be seen that the CFD simulation results obtained using the $k-\omega$ SST Buoyancy model have better accuracy for modeling the wave run-up

phenomenon compared to the modified $k-\omega$ SST Stable turbulence model. Especially at angles of 0° and 45° , the results when using the modified $k-\omega$ SST Stable turbulent model have too high overestimation. However, overall simulation results of the $k-\omega$ SST Buoyancy and modified $k-\omega$ SST Stable turbulence models still produce overprediction and underprediction of the wave run-up phenomenon, which differences may cause by wave reflection and measurement techniques [28].

Table 4. Horizontal force comparison

Horizontal force (F_x)	Force (N)	Error
k-ω SST Buoyancy	4.548	2 %
Modified k-ω SST Stable	4.621	3.63 %
Experiment	4.459	-

Table 3 shows the time inetgral horizontal force data on the monopile during first wave period reaches outlet boundary. It can be seen in table 2, the wave force modeling shows that the results obtained using the turbulent $k-\omega$ SST Buoyancy model have slightly more accurate results with an error of 2% compared to the modified $k-\omega$ SST Stable, which has an error of 3.63%. Therefore, the wave load test on the jack-up production platform hull structure will use the $k-\omega$ SST Buoyancy turbulence model.

5.3 Wave Load on Jack-up Production Platform Hull

In the case of the jack-up platform, data collection was carried out for 30 seconds, more precisely when the waves reached the outlet section at 50 to 80 seconds. In the CFD simulation of the wave load case on the jack-up production platform hull, the $k-\omega$ SST Buoyancy turbulence model is used because the original $k-\omega$ SST turbulence model results in an inappropriate wave modelling, as described previously in Wave Model Verification subsection The data analyzed in this section included the average pressure, vertical force, and horizontal force on the jack-up wall hull platform.

The results of the average pressure value taken are shown in Figure 13. It is known that by varying the direction of the wave arrival, the average pressure value and fluctuations will differ between the variations in the direction of the wave arrival from one to another. The difference in pressure values is due to the different geometric profiles when the waves hit the structure, which causes differences effect of streams of wave flow. Based on the data obtained, the jack-up production platform hull wall with broad surface and relatively facing opposite to the direction of the wave will have a higher value and pressure fluctuation as in the variation of the direction of incidence of 90° and 180° .

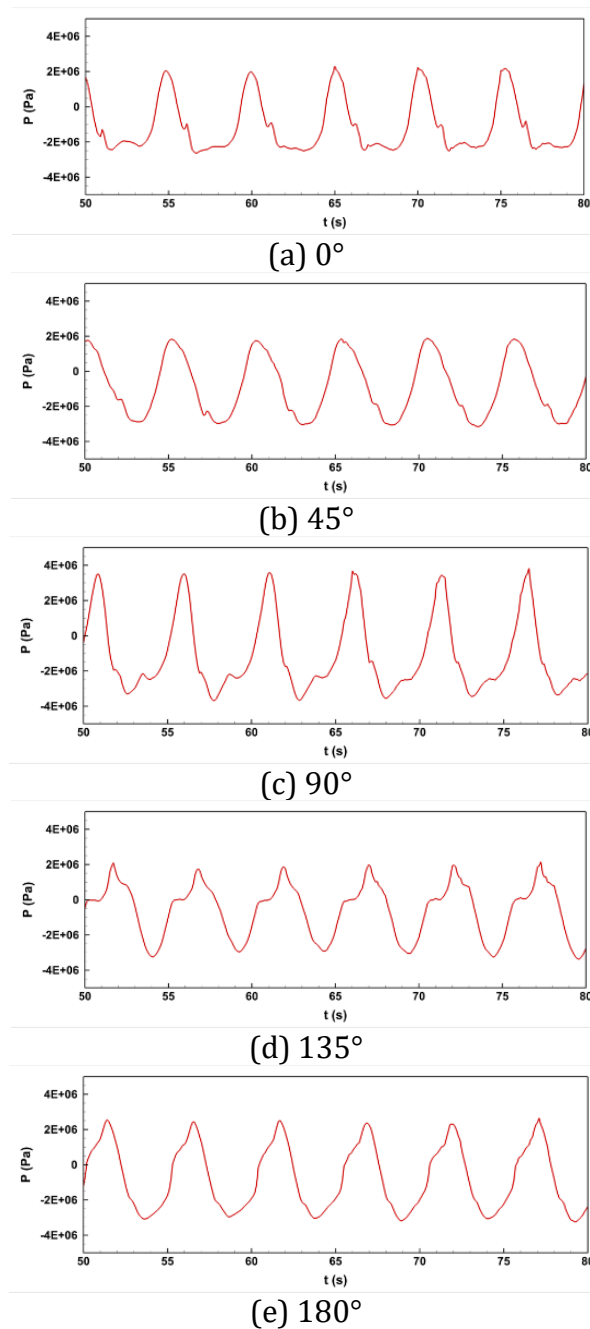


Figure 13. The average pressure value on the walls of the jack-up production platform hull with various wave arrival direction

The high value of pressure in both variations is caused by the absorption of higher wave energy when it hits the larger surface and have relatively facing opposite surface to the direction of the wave incident. In the variation with the direction of wave arrival 45° and 135° relatively have a lower average pressure value because it has a relatively sloping surface side to the direction of the wave incident so that the energy absorbed from the waves is reduced and not evenly distributed. In the variation of the direction

of arrival 0° wave has the same character as the 90° direction of arrival because it has the surface that is relatively facing opposite to the direction of the wave arrival, but the relatively smaller surface area at an angle of 0° causes insignificant pressure fluctuations. In Figure 13, it is also known that the pressure value which has a more significant portion is the negative pressure value, which can be marked by the lines on the pressure curve, which are more negative pressure values. The negative pressure generated is caused by the reflection of the waves that hit the bottom of the jack-up production platform hull, causing the vacuum effect [29].

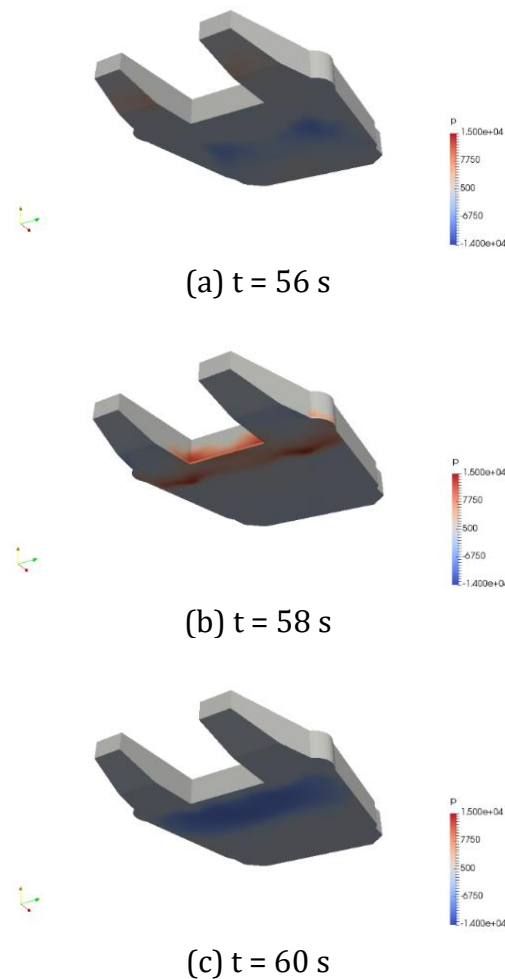


Figure 14. Pressure distribution contours on the jack-up production platform hull walls on the variation of the direction of the wave arrival of 180°

Figure 14 shows pressure distribution contours on the jack-up production platform hull walls on the variation of the direction of the wave arrival of 180° , where the pressure distribution will affect the resultant force on the structure. Figure 14 indicate the value of the negative pressure on the

hull platform jack-up wall has a portion and duration that is more than the positive pressure.

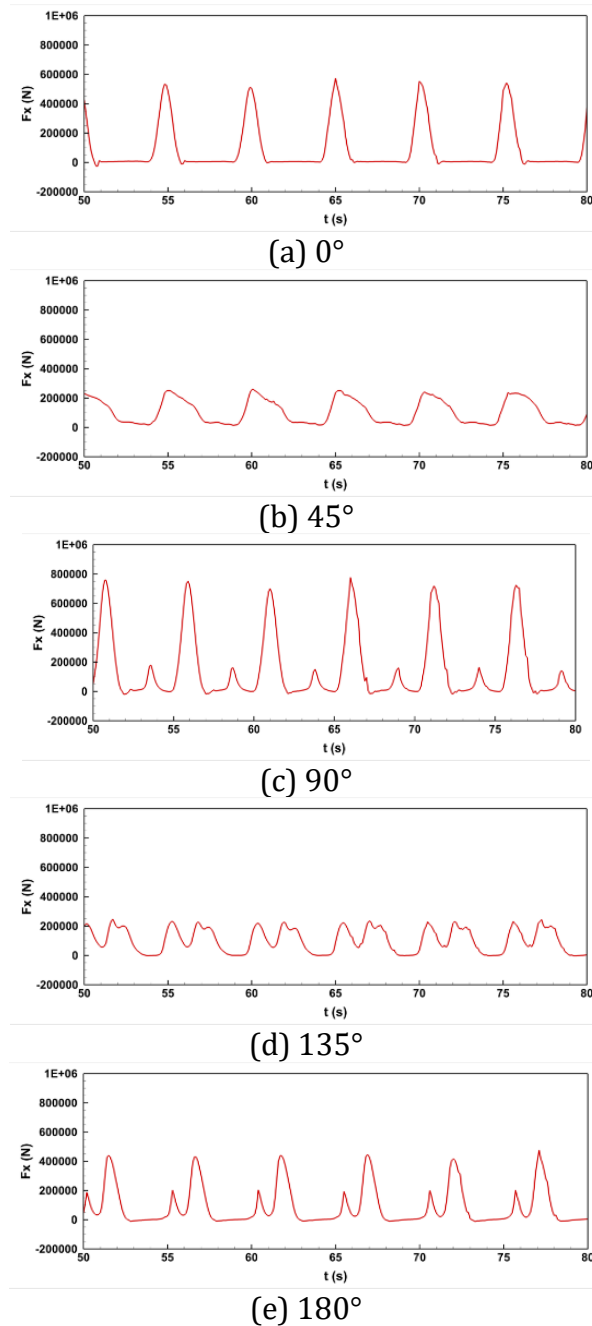


Figure 15. Plot the value of average horizontal force on the jack-up production platform hull wall with various wave arrival direction

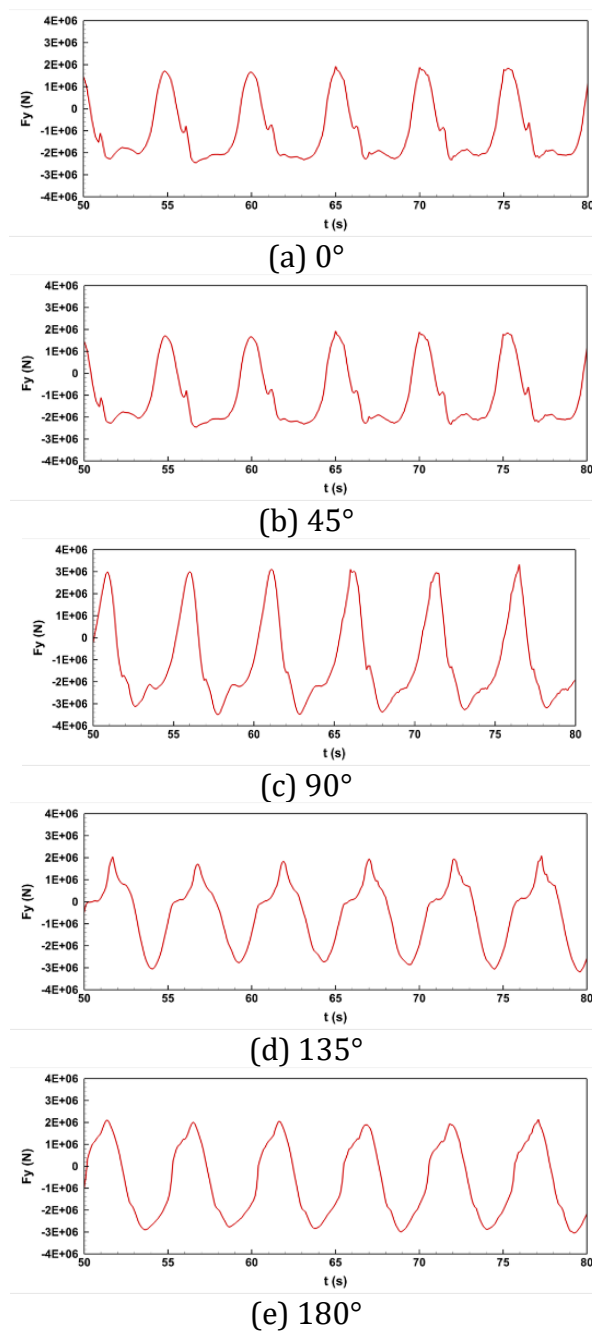


Figure 16. Plot the value of average vertical force on the jack-up production platform hull wall with various wave arrival direction

The plot of the average horizontal force values shown in Figure 15 shows more clearly the effect of the shape of the profile on the formed horizontal force. For variations in the direction of the arrival of waves that are relatively facing opposite to the surface of the jack-up production platform, the hull will have a more prominent horizontal force value because it absorbs more wave energy. The variations in the direction of arrival 0° , 90° , and 180° have a relatively more significant average horizontal force

value than the variations in the direction of arrival 45° and 135° , which have an incident direction relatively oblique to the surface of the platform wall. Especially in the 90° direction of wave arrival, the greatest horizontal force value is obtained compared to other variations because it has the widest impact area surface, which is facing opposite to the direction of the wave incident.

The average vertical force value in Figure 16 shows data with the same character as the pressure data. The most significant average vertical force value is in the variation of the wave arrival direction with a large surface area and relatively facing opposite to the wave arrival direction, which is obtained in variations in the direction of the wave arrival of 90° and 180° . Meanwhile, the direction of arrival of waves with a surface that is relatively, such as variations in the direction of arrival of 45° and 135° , tends to have the smaller vertical force value. The negative vertical force value obtained is directly related to the emergence of the negative pressure value due to the vacuum effect, as shown in Figure 14.

6. CONCLUSION

In this research, the Computational Fluid Dynamic (CFD) was presented using OpenFOAM to analyze the wave load characteristic acting on the jack-up production platform hull structure and also the modification of the k- ω SST turbulent model was applied to accommodate the appropriate wave model. Based on analysis of research data results can be concluded:

1. The k- ω SST Buoyancy turbulence model can effectively reduce the excessive level of turbulence in the surface area compared to the original k- ω SST turbulence model. The verification results of the Stokes V wave model and wave load test on the monopile structure show the relevant results and get an error of 2% from the force load test on the monopile structure compared to the modified k- ω SST Stable that have 3.63% error.
2. Variations in the direction of the waves that produce loads of pressure and force with large values are variations of 0° , 90° , and 180° due to the significant absorption of wave energy because the direction of arrival of waves is relatively facing opposite to the surface of the jack-up production platform hull. Especially in the 90° direction of wave arrival, the greatest wave mean pressure and forces value is obtained compared to other variations because it has the widest impact area surface. While on the other hand, variations with the direction of incidents 45° and 135° , which have a relatively sloping surface with the direction of the wave coming, have lower mean pressure and forces loads due to absorbing lower wave energy.
3. The estimated load generated in this study can be used as a reference in further research involving the structural strength of the jack-up production platform hull.

Nomenclature

u	fluid velocity (m/s)
t	time (s)
ν	kinematic molecular viscosity (kg/ms)
P	kinematic pressure (kg/ms ³)
α	volume fraction
k	turbulent kinetic energy (m ² /s ²)
I	identity tensor
ν_t	turbulent viscosity (m ² /s)
ω	turbulent dissipation rate (1/s)
G_{bk}	buoyancy term (kg/ms ³)
$\bar{\cdot}$	mean component
\cdot'	fluctuating component
\cdot^T	transpose

Acknowledgments

The authors acknowledge to PENS (Politeknik Elektronika Negeri Surabaya) and Cloud Computing Facility in Institut Teknologi Bandung for supporting this research.

REFERENCES

- [1] H. Jessen, **Offshore Oil and Gas Exploitation. Handbook on Marine Environment Protection**, Springer International Publishing (Berlin), pp 683–93, 2017.
- [2] Z. M. Ghazi, I. S. Abbood, F. Hejazi, **Dynamic evaluation of jack-up platform structure under wave, wind, earthquake and tsunami loads**, Journal of Ocean Engineering and Science, vol. 7, pp. 41–57, 2022.
- [3] R. E. Randall, **Elements of ocean engineering**, Society of Naval Architects (Texas), 2010.
- [4] H. Ye, D. Yu, J. Ye, Z. Yang, **Numerical Analysis of Dynamics of Jack-Up Offshore Platform and Its Seabed Foundation under Ocean Wave**, Applied Sciences (Switzerland), vol. 12, pp. 7, 2022.
- [5] R. L. Tawekal, M. Mahendra, D. B. Kurniawan, E. C. Ilman, F. Perdana, Purnawarman FD, **Risk Based Underwater Inspection (RBUI) For Existing Fixed Platforms In Indonesia**, International Journal of Research in Engineering and Science (IJRES), vol. 5, pp. 25-31, 2017.
- [6] K. He, J. Ye, **Dynamics of offshore wind turbine-seabed foundation under hydrodynamic and aerodynamic loads: A coupled numerical way**, Renew Energy, vol. 202, pp. 453–69, 2023.
- [7] E. Mackay, W. Shi, D. Qiao, R. Gabl, T. Davey, D. Ning, **Numerical and experimental modelling of wave interaction with fixed and floating porous cylinders**, Ocean Engineering, vol. 242, pp. 110-118, 2021.

- [8] S. Yan, Q. Li, J. Wang, Q. Ma, Z. Xie, T. Stoesser, **Comparative Numerical Study on Focusing Wave Interaction with FPSO-like Structure**, International Journal of Offshore and Polar Engineering, vol. 29, pp. 149–57, 2019.
- [9] N. R. Arini, S. R. Turnock, M. Tan, **The Effect of Trailing Edge Profile Modifications to Fluid-Structure Interaction of a Vertical Axis Tidal Turbine Blade**, International Journal of Renewable Energy Development, vol. 11, pp. 725–35, 2022.
- [10] M. Nizamani, Z. Nizamani, A. Nakayama, M. Osman, **Analysis of loads caused by waves on the deck near the free surface of the offshore platform using computational fluid dynamics**, Ships and Offshore Structures, vol. 17, pp. 1964–1974, 2022.
- [11] A. Aggarwal, M. A. Chella, H. Bihs, Ø. A. Arntsen, **Numerical study of irregular breaking wave forces on a monopile for offshore wind turbines**, Energy Procedia, vol. 137, pp. 246–254, 2017.
- [12] X. Zeng, W. Shi, C. Michailides, S. Zhang, X. Li, **Numerical and experimental investigation of breaking wave forces on a monopile-type offshore wind turbine**, Renew Energy, vol. 175, pp. 501–519, 2021.
- [13] B. Devolder. **Hydrodynamic modelling of wave energy converter arrays**. Phd Thesis, Ghent University, 2018.
- [14] E. Didier, P. R. F. Teixeira, **Validation and Comparisons of Methodologies Implemented in a RANS-VoF Numerical Model for Applications to Coastal Structures**, J Mar Sci Eng, vol. 10, pp. 9, 2022.
- [15] B. Devolder, P. Rauwoens, P. Troch, **Application of a buoyancy-modified $k-\omega$ SST turbulence model to simulate wave run-up around a monopile subjected to regular waves using OpenFOAM®**, Coastal Engineering, vol. 125, pp. 81–94, 2017.
- [16] B. E. Larsen, D. R. Fuhrman, **On the over-production of turbulence beneath surface waves in Reynolds-averaged Navier–Stokes models**, J Fluid Mech, vol. 853, pp. 419–460, 2018.
- [17] S. Qu, S. Liu, M. C. Ong, **An evaluation of different RANS turbulence models for simulating breaking waves past a vertical cylinder**, Ocean Engineering, vol. 234, pp. 109195, 2021.
- [18] C. Greenshields, **OpenFOAM The OpenFOAM Foundation User Guide**, CFD Direct Ltd, 2011.
- [19] N. G. Jacobsen, D. R. Fuhrman, J. Fredsøe, **A wave generation toolbox for the open-source CFD library: OpenFoam®**, Int J Numer Methods Fluids, vol. 70, pp. 1073–1088, 2012.
- [20] N. U. Azman, M. K. A. Husain, N. I. M. Zaki, E. M. Soom, N. A. Mukhlas, S. Z. A. S. Ahmad, **Structural integrity of fixed offshore platforms by incorporating wave-in-deck**, J Mar Sci Eng, vol. 9, pp. 9, 2012.

- [21] HSE, **HSE Health & Safety Executive Sensitivity of jack-up reliability to wave-in-deck calculation**, MSL Engineering Limited, Report number: 019, 2003.
- [22] M. Métois, M. Benjelloun, C. Lasserre, R. Grandin, L. Barrier, E. Dushi, **Subsidence associated with oil extraction, measured from time-series analysis of Sentinel-1 data: case study of the Patos-Marinza oil field, Albania n.d**, Solid Earth, vol. 11, pp. 363–378, 2020.
- [23] L. De Vos, P. Frigaard, J. De Rouck, **Wave run-up on cylindrical and cone shaped foundations for offshore wind turbines**, Coastal Engineering, vol. 54, pp. 17–29, 2007.
- [24] **ANSYS Fluent Theory Guide**, 2017.
- [25] W. Fan, H. Anglart, **varRhoTurbVOF: A new set of volume of fluid solvers for turbulent isothermal multiphase flows in OpenFOAM**, Comput Phys Commun, vol. 247, pp. 106876, 2020.
- [26] F. R. Menter, **Two-equation eddy-viscosity turbulence models for engineering applications**. AIAA Journal, vol. 32, pp. 1598–1605, 1994.
- [27] American Petroleum Institute (API), **API Recommended Practice 2A-WSD**, ed. 21st. 2007.
- [28] B. Wang, Y. Li, F. Wu, S. Gao, J. Yan, **Numerical Investigation of Wave Run-Up and Load on Fixed Truncated Cylinder Subjected to Regular Waves Using OpenFOAM**, Water (Basel), vol. 14, pp. 2830, 2022.
- [29] T. E. Schellin, M. Perić, O. el Moctar, **Wave-in-deck load analysis for a jack-up platform**, Journal of Offshore Mechanics and Arctic Engineering, vol. 133, pp. 2, 2011.